a simple consequence of the high symmetry (O_h) of this compound. The relative values for the oscillator strength are rather sensitive to a proper description of the metal-ligand and the interligand interaction. Comparing the various compounds $(CO)_5CrR$ (R = CS, PF_3, CHOH), we note that only in the case of R = CS do the low-lying excitations gain some character of the new (R) ligand.

Summary and Conclusions

Gas-phase spectra of metal carbonyls have been measured and assigned. The calculations in this study strongly suggest that the lower lying excitations in these complexes are dominated by metal-to-ligand charge-transfer excitations. In contrast to other calculations discussed in the text, we find no significant 3d-4p contribution to the observed oscillator strength below 6.2 eV (above 200 nm) in any of these complexes. Although 3d-4s excitations are calculated below 6.2 eV, only in the $Fe(CO)_5$ case is there predicted oscillator strength. Insofar as these excitations are local, they are forbidden (g-g). In the case of $Fe(CO)_5$ the band calculated at 292 nm has significant mixing with the allowed 10e' → 11e' metal-to-ligand excitation. Metal d-d excitations are not possible for $Ni(CO)_4$ but are predicted quite low-lying in $Fe(CO)_5$ and $Cr(CO)_6$, comparing well with available experimental data. Although the local nature of these d orbitals again leads to a prediction of no oscillator strength, the d-d band calculated at 430 nm in $Fe(CO)_5$ is (x,y)-allowed ($^1E'$) and should be observable as it is well separated from the next allowed band calculated at 361 nm ($^1A_2''$). The two calculated d-d excitations in $Cr(CO)_6$ at 340 and 300 are formally forbidden, but they are about 1 eV lower in energy than the first allowed band ($^1T_{1u}$ at 269 nm) and have therefore been accessible to UV spectroscopy.

As the INDO model used here has not been parametrized originally for zerovalent metal complexes such as these studied here, more detailed observations of these d-d excitations as well as of ligand-to-metal charge-transfer bands in substituted compounds would greatly help in refining the INDO/S model.

Acknowledgment. This work was supported in part by the Deutsche Forschungsgemeinschaft, the Fonds der Chemischen Industrie, and the Bund der Freunde der TU München. M.C.Z. thanks the members of the Lehrstuhl für Theoretische Chemie for their wonderful hospitality during his visit. We gratefully acknowledge the help and stimulation of Dr. Chris Culberson (Quantum Theory Project, University of Florida), Dipl.-Chem. Peter Knappe (Technische Universität München), and H.-H. Schneider.

Gas-Phase Chemistry of CH_3SOH, $^-CH_2{}^+SHOH$, $CH_3SO^\cdot$, and $^\cdot CH_2SOH$ by Neutralization-Reionization Mass Spectrometry

Frantisek Turecek,* Donald E. Drinkwater, and Fred W. McLafferty*

Contribution from the Chemistry Department, Cornell University, Ithaca, New York 14853-1301.
Received April 10, 1989

Abstract: The kinetically unstable molecules methanesulfenic acid (CH_3SOH, **1**) and its ylide isomer ($^-CH_2{}^+SHOH$, **2**) and the isomeric radicals $CH_3SO^\cdot$ and $^\cdot CH_2SOH$ exist as distinct species in the gas phase. CH_3SOH was generated by flash-vacuum pyrolysis of methyl *tert*-butyl sulfoxide and by neutralization of the corresponding cation radical. The ylide $^-CH_2{}^+SHOH$ was prepared by neutralizaton of the distonic ion, $^\cdot CH_2{}^+SHOH$, generated from di-*n*-butyl sulfoxide by double hydrogen rearrangement. Upon collisional activation CH_3SOH decomposes to $CH_3^\cdot$ and $^\cdot SOH$, while $^-CH_2{}^+SHOH$ affords mainly $^\cdot CH_2SH$ and $^\cdot OH$. Collisionally activated dissociation (CAD) spectra of the corresponding ions also distinguish these $(C,H_4,O,S)^{\cdot+}$ isomers. The isomeric radicals $CH_3SO^\cdot$ and $^\cdot CH_2SOH$ and ions CH_3SO^+ and CH_2SOH^+ were characterized through their neutralization-reionization and CAD mass spectra, respectively. Decomposition mechanisms consistent with deuterium labeling are proposed, and the relative stabilities of the (C,H_4,O,S) isomers are estimated by MNDO calculations.

Sulfenic acids,[1] R-S-OH, represent key reactive intermediates in the biologically important oxidation of thiols[2a,b] and thiolates[2c] to disulfides and sulfur oxyacids. In organic chemistry, sulfenic acids appear as intermediates in double-bond introduction by thermal decomposition of sulfoxides,[3] and synthesis of β-alkylsulfoxyenones.[4] The simplest of these, methanesulfenic acid (CH_3SOH, **1**), presumably plays a role in the photochemical oxidative degradation of methanethiol and dimethyl disulfide,[5] major natural and man-made pollutants.[5d] Investigation and analysis of **1** and other simple sulfenic acids in the condensed phase is hampered by their high propensity to undergo self-condensation to thiosulfinates.[6] Acid **1** has been generated in the gas phase by thermolysis of methyl *tert*-butyl sulfoxide (eq 1) and its structure determined from microwave spectra.[6b,c]

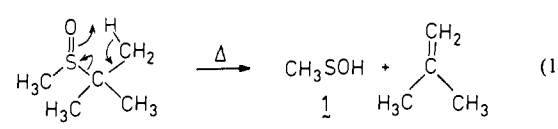

(1)

(1) Hogg, D. R. In *Comprehensive Organic Chemistry*; Barton, D. H. R., Ollis, W. D., Eds.; Pergamon: Oxford, 1979; Vol. 3, Part 11, pp 261-310. For more recent work and leading references see: Davis, F. A.; Jenkins, R. H., Jr.; Rizvi, S. Q. A.; Yocklovich, S. G. *J. Org. Chem.* **1981**, *46*, 3467-3474. Davis, F. A.; Awad, S. B.; Jenkins, R. H., Jr.; Billmers, R. L.; Jenkins, L. A. *J. Org. Chem.* **1983**, *48*, 3071-3074. Davis, F. A.; Billmers, R. L. *J. Org. Chem.* **1985**, *50*, 2593-2595. Davis, F. A.; Jenkins, L. A.; Billmers, R. L. *J. Org. Chem.* **1986**, *51*, 1033-1040.

(2) (a) Capozzi, F.; Modena, G. In *The Chemistry of the Thiol Group, Part 2*; Patai, S., Ed.; Wiley: New York,, 1974; p 785. (b) Allison, W. S. *Acc. Chem. Res.* **1976**, *9*, 293-299. (c) Hogg, D. R.; Rashid, M. A. M. *J. Chem. Res. (S)* **1988**, 160-161.

(3) (a) Trost, B. M.; Salzmann, T. N.; Hiroi, K. *J. Am. Chem. Soc.* **1976**, *98*, 4887-4902. (b) Brown, R. F. C.; Coulston, K. J.; Eastwood, F. W.; Fallon, G. D. *Aust. J. Chem.* **1986**, *39*, 189-193.

(4) (a) Davis, F. A.; Yocklovich, S. G.; Baker, G. S. *Tetrahedron Lett.* **1978**, 97-100. (b) Jones, D. N.; Cottam, P. D.; Davies, J. *Tetrahedron Lett.* **1979**, 4977-4980. (c) Bell, R.; Cottam, P. D.; Davies, J.; Jones, D. N. *J. Chem. Soc., Perkin Trans. 1* **1981**, 2106-2115.

(5) (a) Hatakeyama, S.; Akimoto, H. *J. Phys. Chem.* **1983**, *87*, 2387-2395. (b) Balla, R. J.; Heicklen, J. *J. Photochem.* **1985**, *29*, 297-310. (c) Singleton, D. L.; Irwin, R. S.; Cvetanovic, R. J. *Can. J. Chem.* **1983**, *61*, 968-974. (d) For a review see: Graedel, T. E. *Rev. Geophys. Space Phys.* **1977**, *15*, 421-428.

(6) (a) Kice, J. L.; Cleveland, J. P. *J. Am. Chem. Soc.* **1973**, *95*, 104-109. (b) Block, E., O'Connor, J. *J. Am. Chem. Soc.* **1974**, *96*, 3929-3944. (c) Penn, R. E.; Block, E.; Revelle, L. K. *J. Am. Chem. Soc.* **1978**, *100*, 3622-3623.

0002-7863/89/1511-7696$01.50/0

Table I. CAD/He (30% T) Spectra of $CH_3SOH^{\bullet+}$, $^{\bullet}CH_2{}^{+}SHOH$, $CD_3SOH^{\bullet+}$, and $^{\bullet}CH_2{}^{+}SDOD$

	relative intensity[a]			
m/z	$CH_3SOH^{\bullet+}$ [b]	$^{\bullet}CH_2{}^{+}SHOH$ [c]	$CD_3SOH^{\bullet+}$ [d]	$^{\bullet}CH_2{}^{+}SDOD$ [e]
66			(17)[f]	
65			(92)	(99)
64			1.3	(45)
63	(75)	(65)	1.1	1.6
52				5.5
51				1
50	1.1	10	(75)	57
49	33	32	46	17
48	18	17	(54)	(95)
47	(69)	(72)		(43)
46	(29)	(92)	100	(88)
45	100	100		100
44	16	9.4	16	20
33	5	4	3	9
32	15	26	5	28
15	4.1	2.6		1.1
14	1.7	2.2	0.2	1.5

[a] Peak areas, ±5% relative. Product ion yields relative to the unattenuated precursor ion intensity were: $\mathbf{1}^{\bullet+}$, 0.045; $\mathbf{2}^{\bullet+}$, 0.077; $\mathbf{1}$-$d_3{}^{\bullet+}$, 0.059; $\mathbf{1}$-$d_2{}^{\bullet+}$, 0.085. [b] From dissociative ionization of methyl *n*-propyl sulfoxide at 70 eV. [c] From di-*n*-butyl sulfoxide at 70 eV. [d] From methyl-d_3 *n*-propyl sulfoxide at 70 eV. [e] From di-*n*-butyl-3,3-d_2 sulfoxide at 70 eV. [f] Parentheses indicate values due in part to unimolecular decompositions.

An initial paper[7] reported studies of **1** and its cation radical $\mathbf{1}^{\bullet+}$, including experimental thermochemical data ($\Delta H_f°(\mathbf{1}) = -190$ kJ mol^{-1}, $\Delta H_f°$ ($\mathbf{1}^{\bullet+}$) = 685 kJ mol^{-1})[7] for the evaluation of the reaction enthalpies of decompositions of **1** and $\mathbf{1}^{\bullet+}$. This further study of reaction intermediates, location of transition states, and product structures of the neutrals and corresponding cations utilizes collisionally activated dissociation (CAD),[8] neutralization–reionization,[9] tandem mass spectrometric techniques,[10] and MNDO calculations.[11]

Results and Discussion

Key species in the decomposition of methanesulfenic acid (CH_3SOH, **1**) are its ylide isomer $^{-}CH_2{}^{+}SHOH$ (**2**) and the isomeric radicals $CH_3SO^{\bullet}$ and $^{\bullet}CH_2SOH$. Their structural characterization here is substantially dependent on the characterization of the corresponding cations. Thus, these ions and their unusual gas-phase chemistry will be discussed first.

Ion Decompositions. Cation radical $\mathbf{1}^{\bullet+}$ was produced by electron ionization (EI) of neutral **1** generated as a transient species by flash-vacuum pyrolysis of methyl *tert*-butyl sulfoxide (eq 1),[7] and $\mathbf{1}^{\bullet+}$ was also generated by dissociative ionization (70-eV electrons) of methyl *n*-propyl sulfoxide (eq 2). CAD spectra

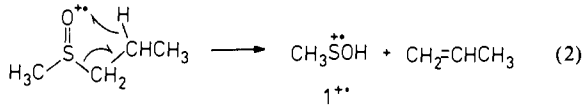

(2)

(Table I)[12] of these ions match closely (correlation coefficient = 0.999)[13] and also match the CAD spectrum for ions prepared by eq 2 dissociative ionization with 15-eV electrons. This provides strong evidence that these ions do have the assigned structure and that they have not undergone appreciable isomerization during these diverse preparations. This is further substantiated (Table I) by the contrasting CAD spectrum of its ylide isomer $^{\bullet}CH_2{}^{+}$-SHOH, $\mathbf{2}^{\bullet+}$ (vide infra).

Table II. Metastable Ion Spectra of $CH_3SOH^{\bullet+}$, $CD_3SOH^{\bullet+}$, $^{\bullet}CH_2{}^{+}SHOH$, and $^{\bullet}CH_2{}^{+}SDOD$[a]

	$CH_3SOH^{\bullet+}$		$CD_3SOH^{\bullet+}$		$^{\bullet}CH_2{}^{+}SHOH$		$^{\bullet}CH_2{}^{+}SDOD$
m/z	rel intensity	$T_{0.5}$	rel intensity	$T_{0.5}$	rel intensity	$T_{0.5}$	rel intensity
66			3[b]	37[b]			
65			12	21			100
64							19
63	30	32[c]			80		
50			100	2.1	3		2
49	4		3		3		2
48			36	3.8			64
47	79	1.8			80	1.9	21
46	100	2.8	5		100	2.6	21
45	7				6		5
33			11				
31	12				11		

[a] Product ion yields were $\sum[l]^+/[M]^{\bullet+} = 0.0023$, 0.0026, and 0.0049 for $CH_3SOH^{\bullet+}$, $CD_3SOH^{\bullet+}$, and $^{\bullet}CH_2S^{+}HOH$, respectively. Relative intensities as integrated peak areas, kinetic energy release ($T_{0.5}$) in kJ mol^{-1}. All major peaks were of a Gaussian type with $n = 2.0$–2.2.[35] [b] Less accurate values due to interference of the precursor ion peak. [c] Composite peak, $n = 1.6$–2.2.[35]

Table III. CAD/He (30% T) and $^{+}NR^{+}$ {Hg (70% T)/O_2 (50% T)} Spectra of CH_3SO^{+} and CH_2SOH^{+}

	relative intensity[a]			
	CAD[b]		$^{+}NR^{+}$ [c]	
m/z	CH_3SO^{+}	$^{+}CH_2SOH$	CH_3SO^{+}	CH_2SOH^{+}
63	...[d]	...[d]	70	26
62	5.3	(28)[e]	4.2	3.7
49	6.5	53	2	13
48	100	54	100	13
47		6	4	2
46	26	(84)[e]	23	67
45	(123)[e]	(446)[e]	61	100
44	15	100	9	34
34	11	4	7	3
33[f]	17	21	11	8
32[f]	23	78	33	29
31	(13)[e]	10	7.1	2.8
29	13	17	7.4	3.9
17		1.3	1.6	5
15	16	0.3	9.1	
14	3.3	6.2	3.3	2.6
13	2	2.7	1.9	3
12	1	1.8	1.5	2.2

[a] Peak areas, relative to the most abundant product ion. [b] Product ion yields were 0.038 and 0.028 for CH_3SO^{+} and CH_2SOH^{+}, respectively. [c] Product ion yields were 0.0057 and 0.0013 for CH_3SO^{+} and CH_2SOH^{+}, respectively. [d] Precursor ions. [e] Also due to unimolecular decompositions. [f] Poorly resolved peaks.

For the gas-phase chemistry of the $(C,H_4,O,S)^{\bullet+}$ ions indicated by these spectra, the lowest energy processes are shown in the metastable ion (MI) spectra (Table II, lifetimes 14–17 μs). The loss of hydrogen involves two pathways (eq 3), giving rise to a

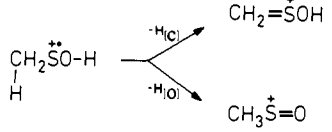

(3)

composite peak from their different values of kinetic energy release; for $CD_3SOH^{\bullet+}$, $\mathbf{1}$-$d_3{}^{\bullet+}$, the narrower (smaller energy) and more abundant component corresponds to the loss of deuterium. The relative intensities for this loss are sensitive to CAD, showing a 50-fold increase in $[M - H,D]^{+}$ on increasing the pressure from

(7) Turecek, F.; Brabec, L.; Vondrak, T.; Hanus, V.; Hajicek, J.; Havlas, Z. *Collect. Czech. Chem. Commun.* **1988**, *53*, 2140–2158.
(8) (a) McLafferty, F. W.; Bente, P. F., III; Kornfeld, R.; Tsai, S.-C.; Howe, I. *J. Am. Chem. Soc.* **1973**, *95*, 2120. (b) McLafferty, F. W.; Kornfeld, R.; Haddon, W. F.; Levsen, K.; Sakai, I.; Bente, P. F., III; Tsai, S.-C.; Schuddemage, H. D. R. *J. Am. Chem. Soc.* **1973**, *95*, 3886.
(9) (a) Gellene, G. I.; Porter, R. F. *Acc. Chem. Res.* **1983**, *16*, 200–207. (b) Danis, P. O.; Wesdemiotis, C.; McLafferty, F. W. *J. Am. Chem. Soc.* **1983**, *105*, 7454–7457. For recent reviews see: (c) Wesdemiotis, C.; McLafferty, F. W. *Chem. Rev.* **1987**, *87*, 485–500. (d) Terlouw, J. K.; Schwarz, H. *Angew. Chem., Int. Ed. Engl.* **1987**, *26*, 805–815.
(10) McLafferty, F. W., Ed. *Tandem Mass Spectrometry*; Wiley: New York, 1983.
(11) Dewar, M. J. S.; Thiel, W. *J. Am. Chem. Soc.* **1977**, *99*, 4899–4907.
(12) Full data are available as Supplementary Material.
(13) Shorter, J. *Correlation Analysis of Organic Reactivity*; Research Studies Press, Wiley: Chichester, 1982.

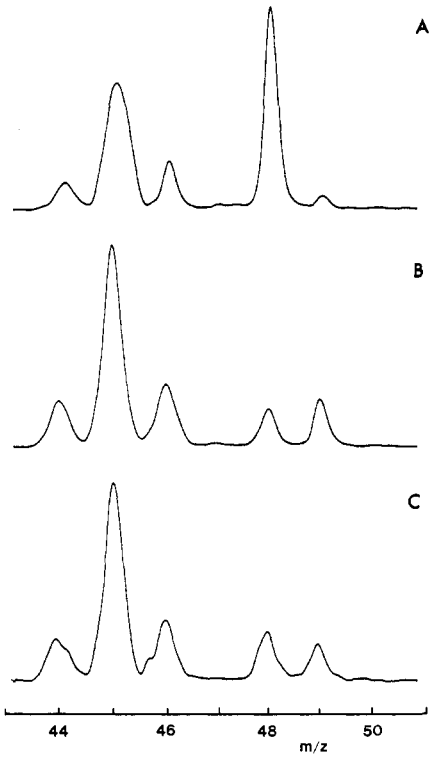

Figure 1. CAD(He, 30% T) spectra of (A) CH_3SO^+, (B) CH_2S^+OH, and (C) $(M - H)^+$ from $\mathbf{1}^{\bullet+}$.

2.5×10^{-7} to 1.2×10^{-6} Torr. However, this causes little change in the $[M - D]^+/[M - H]^+$ value (84:16, Table II), suggesting that the hydrogen loss in the MI spectrum is due to residual CAD. To check this value, the proportion of the isomeric $(C,H_3,O,S)^+$ ions (eq 3) was determined from their CAD spectra (Table III).

CH_3SO^+ from dissociative ionization of dimethyl sulfoxide[14] undergoes facile C–S bond cleavage to produce abundant $SO^{\bullet+}$, m/z 48, and CH_3^+ secondary fragments. The CAD spectrum of $CH_2{=}SOH^+$, generated from di-*n*-butyl sulfoxide via *n*-butanesulfenic acid (eq 4) shows $CH_2^{\bullet+}$ (m/z 14) and ^+SOH (m/z 49)

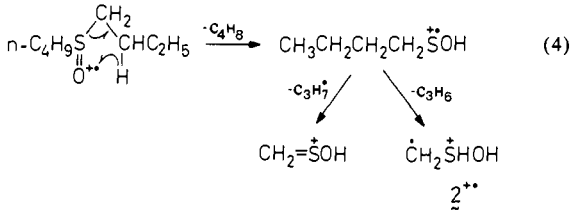

(4)

as more prominent fragments, while CH_3^+ is almost absent. The $(M - H)^+$ from $\mathbf{1}^{\bullet+}$ was characterized in an MS/MS/MS experiment;[10,15] MS-I selected ions $\mathbf{1}^{\bullet+}$ from methyl *n*-propyl sulfoxide were subjected to CAD, the resulting $(M - H)^+$ ions selected by kinetic energy and subjected to CAD, followed by mass analysis. The resulting spectrum (Figure 1) resembles that of $CH_2{=}SOH^+$; integrated peak intensities and CAD efficiencies indicate 91% $CH_2{=}SOH^+$ and 9% CH_3SO^+. This compares well with $[M - D]^+/[M - H]^+ = 84/16$ from the CAD spectrum of $CD_3SOH^{\bullet+}$ (Table I), which should be lowered by the isotope effect favoring H loss. The preferential loss of the carbon-bound hydrogen atoms is consistent with thermochemical data. The threshold energy for $\mathbf{1}^{\bullet+} \rightarrow CH_3SO^+ + H^\bullet$ is calculated as $E_{TH} = 954$ kJ mol^{-1}, based on $\Delta H_f(CH_3SO^+) = 736$ kJ mol^{-1},[16] and $\Delta H_f(H^\bullet) = 218$ kJ mol^{-1}.[17] The threshold energy for $\mathbf{1}^{\bullet+} \rightarrow$

Scheme I

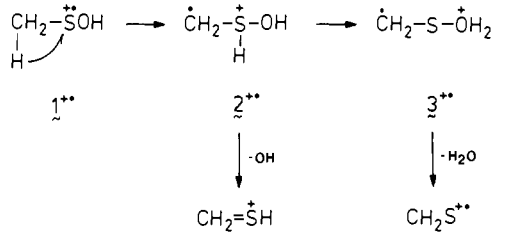

Scheme II

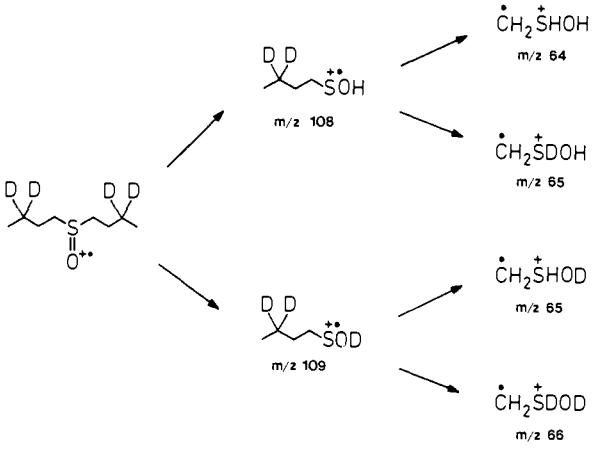

$CH_2{=}SOH^+ + H^\bullet$ can be estimated as $E_{TH} \geq 877$ kJ mol^{-1} from the $\Delta H_f°(\mathbf{1}^{\bullet+})$ and the dissociation energy of the C–H bond in the related $CH_3SH^{\bullet+}$ (192 kJ mol^{-1}).[17,18] In addition, the O–H bond cleavage in $\mathbf{1}^{\bullet+}$ may involve a substantial reverse activation energy, by analogy with the H loss from $R\text{–}OH^{\bullet+}$ ions.[19]

Of the other $\mathbf{1}^{\bullet+}$ dissociations, loss of hydroxyl gives rise to CH_2SH^+, as shown by comparing the CAD spectrum of the latter with that from 2-hydroxyethanethiol.[12,20] The loss of $OH^\bullet$ is not preceded by hydrogen scrambling in metastable $\mathbf{1}^{\bullet+}$; in the MI spectrum of $\mathbf{1}$-$d_3^{\bullet+}$ (Table II) m/z 47 shifts cleanly to m/z 50, CD_2SD^+. Similarly, the loss of water from $\mathbf{1}^{\bullet+}$, involving the hydroxyl group and another hydrogen, shows a clean mass shift of m/z 46 to 48. Both the formation of CH_2SH^+ and of $CH_2S^{\bullet+}$ require that specific hydrogen transfers occur in $\mathbf{1}^{\bullet+}$; Radom's mechanism[21] for $CH_3SCH_3^{\bullet+} \rightarrow {}^\bullet CH_2{}^+SHCH_3 \rightarrow CH_2SH^+$ suggests that $\mathbf{1}^{\bullet+}$ first rearranges to the ylidion $\mathbf{2}^{\bullet+}$ which can then yield $CH_2{=}SH^+$ (Scheme I). A further hydrogen migration from sulfur to oxygen forming another distonic[21] intermediate ($\mathbf{3}^{\bullet+}$) would lead to $CH_2S^{\bullet+}$ and H_2O; the latter rearrangement must be irreversible to account for the absence of hydrogen exchange. Consistent with this additional rearrangement, there is a large deuterium isotope effect, reducing the formation of $CH_2S^{\bullet+}$ versus that of CH_2SH^+. Further, these formations are competitive in the metastable time region, despite the more favorable threshold energy (764 kJ mol^{-1})[17] for $CH_2S^{\bullet+}$ formation versus that (901 kJ mol^{-1})[17] for CH_2SH^+ formation.

To substantiate the intermediacy of $\mathbf{2}^{\bullet+}$ (Scheme I), this isomer was generated from di-*n*-butyl sulfoxide by double hydrogen rearrangement (eq 4). The significant $HSOH^{\bullet+}$ (m/z 50) and large $(M - H_2O)^{\bullet+}$ (m/z 46) peaks in its CAD spectrum (Table I) are consistent with the ylide structure $\mathbf{2}^{\bullet+}$ and its existence as a distinct

(14) Potzinger, P.; Stracke, H. V.; Kupper, W.; Gollnick, K. *Z. Naturforsch., Teil A* **1975**, *30*, 340–346.
(15) Feng, R.; Wesdemiotis, C.; Baldwin, M. A.; McLafferty, F. W. *Int. J. Mass Spectrom. Ion Processes* **1988**, *86*, 95–107.
(16) Zha, Q.; Nishimura, T.; Meisels, G. G. *Int. J. Mass Spectrom. Ion Processes* **1988**, *83*, 1–12.
(17) Lias, S. G.; Bartmess, J. E.; Liebman, J. F.; Holmes, J. L.; Levin, R. D.; Mallard, W. G. *J. Phys. Chem. Ref. Data* **1988**, *17*, Suppl. 1.
(18) Butler, J. J.; Baer, T.; Evans, S. A., Jr. *J. Am. Chem. Soc.* **1983**, *105*, 3451–3455.
(19) Burgers, P. C.; Holmes, J. L.; Terlouw, J. K. *J. Chem. Soc., Chem. Commun.* **1984**, *642*–643.
(20) Dill, J. D.; Fisher, C. L.; McLafferty, F. W. *J. Am. Chem. Soc.* **1979**, *101*, 6526–6531.
(21) Yates, B. F.; Bouma, W. J.; Radom, L. *J. Am. Chem. Soc.* **1984**, *106*, 5805–5808.

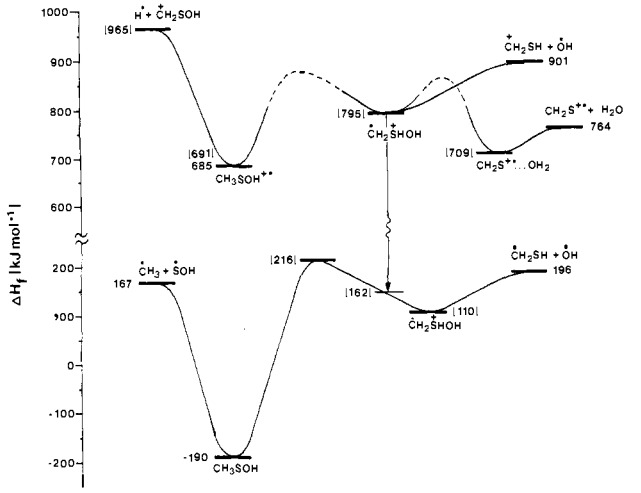

Figure 2. Potential energy diagram for decompositions and isomerizations of **1**, **2**, $\mathbf{1}^{\bullet+}$, and $\mathbf{2}^{\bullet+}$. Parentheses indicate values from MNDO calculations.

stable species.[22] The MI spectrum of $\mathbf{2}^{\bullet+}$ shows $CH_2S^{\bullet+}$ and CH_2SH^+ abundances closely similar to those of $\mathbf{1}^{\bullet+}$ (Table II), consistent with the intermediacy of $\mathbf{2}^{\bullet+}$ in these decompositions, as suggested above by the MI/CAD data of **1**-d_3.

To assess the reversibility of the $\mathbf{1}^{\bullet+} \rightarrow \mathbf{2}^{\bullet+}$ isomerization, labeled **2** analogues were prepared from di(butyl-3,3-d_2) sulfoxide (Scheme II). However, the loss of butene produces both $CH_3CD_2CH_2CH_2SOH^{\bullet+}$ and $CH_3CD_2CH_2CH_2SOD^{\bullet+}$ (100:76), so of the subsequent fragmentation products (CH_2SOH^+, 100%; CH_2SOD^+ + $^{\bullet}CH_2{}^+SHOH$, 90%; $^{\bullet}CH_2{}^+SHOD$ + $^{\bullet}CH_2{}^+SDOH$, 59%; and $^{\bullet}CH_2{}^+SDOD$, m/z 66, 40%) only the last is useful. The CAD and MI spectra (Tables I and II) of $^{\bullet}CH_2{}^+SDOD$ (**2**-$d_2^{\bullet+}$) exhibit both $CH_2S^{\bullet+}$ and $CHDS^{\bullet+}$;[23] because the hydroxyl deuterium atom does not migrate (vide supra), the reaction $\mathbf{1}^{\bullet+} \rightleftarrows \mathbf{2}^{\bullet+}$ must be reversible (eq 5). The H/D exchange is incomplete,

$$\begin{array}{ccc} \dot{C}H_2\dot{S}DOD & \rightleftharpoons & CH_2D\dot{S}\dot{O}D \rightleftharpoons \dot{C}HD\dot{S}HOD \\ \downarrow & & \downarrow \\ CH_2S^{\bullet+} + D_2O & & CHDS^{\bullet+} + HOD \end{array} \quad (5)$$

with $[CH_2S^{\bullet+}]/[CHDS^{\bullet+}]$ = 1:1 in the MI spectrum, suggesting that the $\mathbf{2}^{\bullet+} \rightarrow \mathbf{1}^{\bullet+}$ isomerization is competitive with the loss of hydroxyl and elimination of water in the metastable time window. However, the CAD spectrum of **2**-$d_2^{\bullet+}$ (Table I) shows a dominant mass shift of m/z 50 to 52, indicating that the isomerization is less competitive at higher energies.

The relative energies of $\mathbf{1}^{\bullet+}$, $\mathbf{2}^{\bullet+}$, and $\mathbf{3}^{\bullet+}$ estimated from MNDO calculations are displayed in Figure 2 (values in parentheses). MNDO reproduces very well the experimental $\Delta H_f°$ of $\mathbf{1}^{\bullet+}$, and finds $\mathbf{2}^{\bullet+}$ as a stable structure in a potential-energy minimum, destabilized against $\mathbf{1}^{\bullet+}$ by 104 kJ mol^{-1}. This is consistent with the general destabilization of sulfur ylidions, e.g., ΔE = 86 kJ mol^{-1} for $^{\bullet}CH_2SH_2^+$ versus $CH_3SH^{\bullet+}$.[21,24] In contrast, $\mathbf{3}^{\bullet+}$ is calculated to exist as an ion–molecule complex with a long S–O bond (0.319 nm) and a small C–S–O bond angle (90°), and its decomposition to $CH_2S^{\bullet+}$ and H_2O is only slightly endothermic (Figure 2). Thus $\mathbf{3}^{\bullet+}$ should be produced from $\mathbf{2}^{\bullet+}$ with more internal energy than that required for decomposition,

Table IV. Neutralization–Reionization ($^+NR^+$) {Hg (90% T)/O_2 (50% T)} and Neutralization–Collisional Activation–Reionization ($^+NCR^+$) {Hg (90% T)/He (50% T)/O_2 (50% T)} Mass Spectra of $\mathbf{1}^{\bullet+}$ and $\mathbf{2}^{\bullet+}$

	relative intensity[a]			
	$CH_3SOH^{\bullet+}$ ($\mathbf{1}^{\bullet+}$)		$^{\bullet}CH_2{}^+SHOH$ ($\mathbf{2}^{\bullet+}$)	
m/z	$^+NR^+$	$^+NCR^+$	$^+NR^+$	$^+NCR^+$
64	34	25	26	17
63	7.8	4.3	5.6	3.5
62	0.5	0.4	0.2	0.2
50	0.4	0.5	1.6	2
49	5.5	11	5.7	5.7
48	5.1	7.2	4.1	3.6
47	11	9.2	12	15
46	6.5	6.5	11	19
45	14	17	15	11
44	3.8	4.7	2.7	3.4
34	0.8	0.9	0.7	1.3
33[b]	2	1.7	1.6	1.6
32[b]	5.4	8.7	6.5	8.5
31[b]	0.9	0.6	1.1	1
29	0.6		1.1	1.3
17	0.5	0.7	1	1.2
16	0.2	0.2	0.5	0.6
15	1.1	1.0	1.1	0.9
14	0.6	0.5	0.9	1.1
13	0.3	0.4	0.8	0.7
12	0.2	0.2	0.5	0.4

[a] Peak areas, relative to the sum of product ion intensities. Product ion yields were: $^+NR^+$, 0.0012 and 0.0013 for $\mathbf{1}^{\bullet+}$ and $\mathbf{2}^{\bullet+}$, respectively; $^+NCR^+$, 0.00028 and 0.00045 for $\mathbf{1}^{\bullet+}$ and $\mathbf{2}^{\bullet+}$, respectively. [b] Poorly resolved peaks.

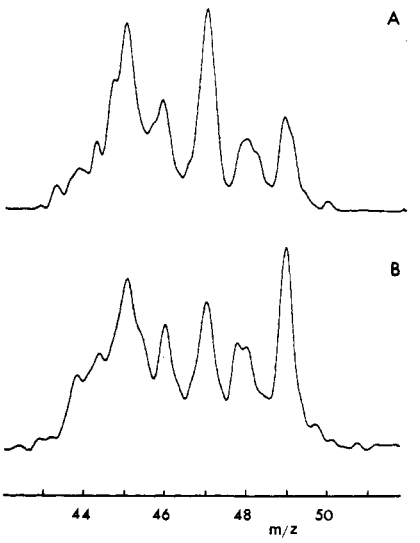

Figure 3. $^+NR^+$ {Hg(90% T)/O_2(50% T)} (A), and $^+NCR^+$ {Hg (90% T)/He(50% T)/O_2 (50% T)} (B) spectra of $\mathbf{1}^{\bullet+}$.

consistent with the clean loss of HDO from **1**-$d_3^{\bullet+}$ via $^{\bullet}CD_2S^+$-OHD (vide supra). The tentative barriers to the isomerizations of Figure 2 conform to the kinetics of decomposition and isomerization discussed above.

Neutral Decompositions of CH_3SOH and $^{\bullet}CH_2{}^+SHOH$. Ions $\mathbf{1}^{\bullet+}$ and $\mathbf{2}^{\bullet+}$ (in a mixture with $\mathbf{1}^{\bullet+}$) have further been used to generate the corresponding neutral species by electron capture from a target gas.[25] Neutralization with mercury at high ion transmittance (single collision conditions)[26] followed by reionization with oxygen resulted in high recovery of undecomposed parent ions $\mathbf{1}^{\bullet+}$ and $\mathbf{2}^{\bullet+}$ (Table IV). The surviving $\mathbf{1}^{\bullet+}$ shows a higher relative abundance compared to $\mathbf{2}^{\bullet+}$. The $^+NR^+$ spectra

(22) The homologous $^{\bullet}CH_2S^+(CH_3)OH$ ion has recently been found as a stable species in the gas phase: Carlsen, L.; Egsgaard, H. *J. Am. Chem. Soc.* **1988**, *110*, 6701–6705.

(23) In the CAD spectrum of **2**-$d_2^{\bullet+}$ m/z 47 can only be $CHDS^{\bullet+}$, while m/z 46 is $CH_2S^{\bullet+}$ and/or CDS^+; the presence of CDS^+ in addition to CHS^+ (m/z 45) would also demonstrate the reversibility of $\mathbf{1}^{\bullet+} \rightleftarrows \mathbf{2}^{\bullet+}$.

(24) (a) Yates, B. F.; Bouma, W. J.; Radom, L. *Tetrahedron* **1986**, *42*, 6225–6234. (b) Radom, L.; Bouma, W. J.; Nobes, R. H.; Yates, B. F. *Pure Appl. Chem.* **1984**, *56*, 1831–1842.

(25) (a) Danis, P. O.; Feng, R.; McLafferty, F. W. *Anal. Chem.* **1986**, *58*, 348–354. (b) Danis, P. O.; Feng, R.; McLafferty, F. W. *Anal. Chem.* **1986**, *58*, 355–358.

(26) Todd, P. J.; McLafferty, F. W. *Int. J. Mass Spectrom. Ion Phys.* **1981**, *38*, 371–378.

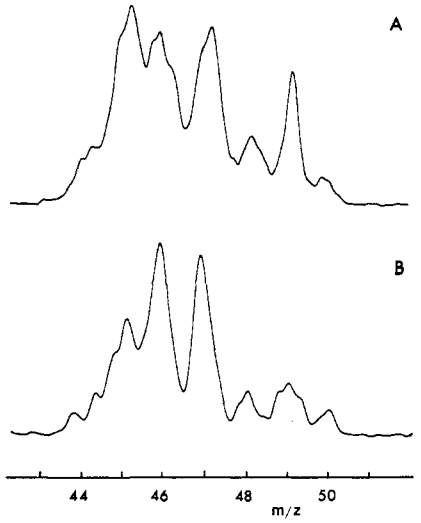

Figure 4. $^{+}NR^{+}$ (A) and $^{+}NCR^{+}$ (B) spectra of $2^{\bullet+}$. Collision conditions as in Figure 3.

Table V. MNDO Heats of Formation and HOMO Energies of (C, H_4, O, S) Isomers

structure	$\Delta H_f°$ (kJ mol^{-1})	$-\epsilon_{HOMO}$ (eV)
$HO-CH_2-SH$	−217	10.07
CH_3-S-OH	−179	9.39
CH_3-O-SH	−120	9.87
$CH_3-S^{+}H-O^{-}$	41	10.13
$CH_3-O^{+}H-S^{-}$	70	8.00
$^{-}CH_2-S^{+}H-OH$	110	8.20
$^{-}CH_2-O^{+}H-SH$	183	7.72
$^{-}CH_2-S-O^{+}H_2$	...[a]	
$^{-}CH_2-O-S^{+}H_2$	...[b]	

[a] Unstable, decomposes spontaneously to CH_2S and H_2O. [b] Unstable, decomposes spontaneously to CH_2O and H_2S.

of $1^{\bullet+}$ and $2^{\bullet+}$ further differ in the relative abundances of fragments at m/z 50, 46, and 14, similar to the differences in the CAD spectra. Decompositions of ionic and neutral species were distinguished by a neutralization–collisional activation–reionization experiment;[15] mass-selected precursor ions were neutralized with mercury vapor and the selected fast neutrals activated by collisions with helium. After second deflection of ions possibly formed in this step, the resulting mixture of neutrals was reionized by collisions with oxygen and analyzed. The $^{+}NCR^{+}$ spectra (Table IV) show pronounced changes (Figures 3 and 4). With **1** the collisional activation promotes formation of •SOH and S. The former species is a primary product of decomposition of **1** (Figure 2), showing that cleavage of the C–S bond is favored in the neutral molecule, in contrast to the ion. This is compared to the pyrolytic decomposition of **1** which yields mostly CH_2S, possibly via surface-catalyzed elimination of water.[6c] Collisional activation of **2** promotes formation of $^{\bullet}CH_2SH$ and CH_2S, resulting from S–O bond cleavage and, with the latter, hydrogen migration. Note that with **1** the relative abundance of CH_2SH *decreases* upon $^{+}NCR^{+}$, while that of CH_2S does not change. The $^{+}NCR^{+}$ spectra (Figures 3 and 4) clearly distinguish neutral isomers **1** and **2** and bring additional evidence that ylide **2** is stable on the timescale of the experiment ($\approx 10^{-6}$ s).

The relative stabilities of **1**, **2**, and some other isomers were estimated by MNDO calculations (Table V). **1** is the second most stable (C, H_4, O, S) isomer, while the calculated $\Delta H_f°$ agrees well with the experimental value. Despite having a substantially higher $\Delta H_f°$ value, **2** is calculated as a stable equilibrium structure.[12] The energy barrier to decomposition to $^{\bullet}CH_2SH$ and •OH could not be obtained reliably by MNDO since the method severely underestimated the heats of formation of the products. Interestingly, there is no stable equilibrium structure for **3** which will decompose without barrier to CH_2S and H_2O, for which MNDO gives accurate heats of formation.

Table VI. Thermochemical Data for Decompositions of **1** and **2**

reactant	products	ΔH_r[a]
1	$^{\bullet}CH_2SOH + H^{\bullet}$	(398)
	$CH_3SO^{\bullet} + H^{\bullet}$	341
	$CH_3^{\bullet} + {}^{\bullet}SOH$	357
	$CH_3S^{\bullet} + {}^{\bullet}OH$	368
2	$CH_2 + HSOH$	(334)
	$^{\bullet}CH_2SOH + H^{\bullet}$	(98)
	$^{\bullet}CH_2SH + {}^{\bullet}OH$	(86)
	$CH_2S + H_2O$	(−247)

[a] From thermochemical data.[30,31] Estimated and MNDO-based values in parentheses.

The ability of neutral **2** to survive is surprising in view of an unfavorable Franck–Condon factor.[27] MNDO calculations give very different equilibrium geometries for **2** and $2^{\bullet+}$; the neutral molecule has a typical ylide structure[28] showing a short C–S bond (0.159 nm) and a long S–O bond (0.165 nm), and having the CH_2 group twisted by 71° out of the C–S–O plane. The molecule is highly polarized; net atomic charges are calculated as −0.85 (C), 1.09 (S), −0.52 (O), 0.21 ($H_{(O)}$), and −0.1 ($H_{(S)}$). In contrast, $2^{\bullet+}$ is calculated to possess a long C–S bond (0.171 nm), while the S–O bond is somewhat shorter (0.161 nm) than in **2**. The CH_2 group lies close to the C–S–O plane ($\theta = -6°$). Hence, it follows that upon vertical neutralization (time of interaction, $t = 5 \times 10^{-15}$ s) **2** is produced in an excited state. According to MNDO, the potential energy of **2** formed with the initial equilibrium geometry of $2^{\bullet+}$ is at 162 kJ mol^{-1}, i.e., 52 kJ mol^{-1} above that of the ground state. By comparison, the barrier to isomerization **2** → **1** was calculated as 106 kJ mol^{-1} above the ground-state energy of **2**, so the latter ylide is predicted to be stable even if formed with a nonequilibrium geometry (Figure 2).[24] Although the MNDO energy data should be treated as rough estimates, qualitatively they account for the behavior of **1** and **2**. The existence of the latter and its distinct fragmenation upon collisional activation show that structure **2** represents a potential energy minimum separated from that of **1** by an energy barrier higher than those for dissociations (Figure 2).

The thermochemistry of the neutral decompositions can be assessed by using the known or estimated heats of formation of the products (Table VI).[29] The lowest energy, simple-bond, cleavage in **1** corresponds to the formation of $CH_3SO^{\bullet}$ and $H^{\bullet}$. In contrast, CAD of **1** favors the formation of $CH_3^{\bullet}$ and •SOH (Figure 2). This discrepancy can be due to a reversed order of the actual reaction endothermicities in view of the relatively large error margins in the estimates of the $\Delta H_f°$ of $CH_3SO^{\bullet}$ and •SOH.[31] Alternatively, the homolytic cleavage of the O–H bond in **1** may involve an activation barrier.

The cleavage of the S–O bond in **2** is favored over loss of the sulfur hydrogen atom in agreement with the CAD results. Simultaneously, **2** is metastable with respect to highly exothermic decomposition to CH_2S and H_2O, which is likely to proceed via the unstable $^{-}CH_2S^{+}OH_2$ (Table VI). Both the existence of **2** and the competition with the endothermic decomposition to $^{\bullet}CH_2SH$ and •OH indicate that the isomerization **2** →

(27) Wesdemiotis, C.; Feng, R.; Williams, E. R.; McLafferty, F. W. *Org. Mass Spectrom.* **1986**, *21*, 689–695.

(28) Eades, R. A.; Gassman, P. G.; Dixon, D. A. *J. Am. Chem. Soc.* **1981**, *103*, 1066–1068.

(29) $\Delta H_f°$ (kJ mol^{-1}): $H^{\bullet}$ (218),[17] $CH_3^{\bullet}$(146),[32] $OH^{\bullet}$(39),[17] SO(5),[17] $^{\bullet}CH_2SOH$ (-10, estimated from BDE(H--CH_2SOH) ≈ 398 kJ mol^{-1}),[30] $CH_3SO^{\bullet}$(-67),[31] •SOH(21),[31] $CH_3S^{\bullet}$(139),[31] $^{\bullet}CH_2SH$ (157, estimated from BDE(H--CH_2SH) ≈ 398 kJ mol^{-1} and $\Delta H_f°(CH_3SH) = -23$ kJ mol^{-1}),[31,32] CH_2S (105),[17] H_2O (−242),[17] HSOH (54, estimated from $\Delta H_f°$(•SOH),[31] and BDE(H--SOH) ≈ 293 kJ mol^{-1}),[31] CH_2 (390).[17]

(30) McMillen, D. F.; Golden, D. M. *Annu. Rev. Phys. Chem.* **1982**, *33*, 493–532.

(31) Benson, S. W. *Chem. Rev.* **1978**, *78*, 23–35.

(32) Pedley, J. B.; Rylance, J. *Sussex N.P.L. Computer Analyzed Thermochemical Data; Organic and Organometallic Compounds*; University of Sussex: Sussex, 1977.

Scheme III

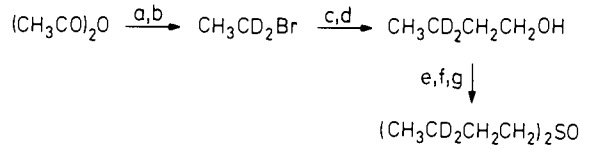

[a] $LiAlD_4$, THF, reflux 4h. [b] HBr. [c] Mg, Et_2O. [d] Oxirane (2.2 equiv), 0 °C. [e] HBr. [f] Na_2S, C_6H_6/H_2O, $C_6H_5CH_2N^+Et_3 \cdot Cl^-$. [g] $NaIO_4$, $MeOH/H_2O$.

$^-CH_2S-^+OH_2 \rightarrow CH_2S + H_2O$ must overcome an activation barrier.

Radicals $CH_3SO^\bullet$ and $^\bullet CH_2SOH$. The existence of noninterconverting ions CH_3SO^+ and $CH_2{=}SOH^+$ prompted us to prepare the corresponding radicals, $CH_3SO^\bullet$ and $^\bullet CH_2SOH$, and examine their reactivities. The $^+NR^+$ spectrum of CH_3SO^+ (Table III) shows abundant recovered parent ions and increased relative intensities of $SO^{\bullet+}$ (m/z 48), $CH_2S^{\bullet+}$ (m/z 46), and $S^{\bullet+}$ (m/z 32). $CH_2{=}SOH^+$ affords a different $^+NR^+$ spectrum (Table III). The recovered parent ion is less abundant than with CH_3SO^+, indicating lower kinetic or thermodynamic stability of $^\bullet CH_2SOH$, compared with $CH_3SO^\bullet$.[29] The $^+NR^+$ spectrum of CH_2SOH^+ further reveals an increased signal of $CH_2S^{\bullet+}$ which is attributed to neutral decomposition of lowest energy, $^\bullet CH_2SOH \rightarrow CH_2S + OH^\bullet$ (E_{TH} = 144 kJ mol^{-1}).[29] The occurrence of $CH_2S^{\bullet+}$ in the $^+NR^+$ spectrum of CH_3SO^+ may indicate isomerization of excited $CH_3SO^\bullet$ to $^\bullet CH_2SOH$. In order to compete with decomposition to $CH_3^\bullet$ and SO (E_{TH} = 151 kJ mol^{-1}), the isomerization is likely to overcome a substantial activation barrier.

Conclusions

The isomeric molecules CH_3SOH and $^-CH_2{}^+SHOH$, and radicals $CH_3SO^\bullet$ and $^\bullet CH_2SOH$, were generated by neutralization of the corresponding ions and shown to survive for $\geq 10^{-6}$ s. The $^+NCR^+$ mass spectra appear to be very useful for distinguishing isomeric ions or mixtures thereof through specific decompositions of the corresponding neutral species.

Experimental Section

Measurements were made with a tandem mass spectrometer described previously,[33] consisting of a Hitachi RMH-2 double-focusing mass spectrometer as the first mass analyzer (MS-I), a special collision region furnished with three collision cells,[15] an electrostatic analyzer as MS-II and a second magnet as MS-III, or the last as MS-II. For $^+NR^+$ mass spectra,[9b,25] the ions produced at 70-eV electron energy and accelerated to 9.9 keV are selected by MS-I and allowed to undergo charge-exchange neutralization in the first collision cell.[25a] The remaining ions are deflected electrostatically, and the resulting fast neutrals are reionized in the second collision cell.[25b] For $^+NCR^+$ mass spectra, the selected neutrals exiting from the first collision cell undergo collisions with helium (50% transmittance) in the second collision cell; the ions formed are deflected electrostatically and the remaining neutrals reionized by collisions with oxygen (50% transmittance) in the third collision cell.[15] For MS/MS/MS experiments, the ions selected by MS-I undergo collisions with oxygen (50% transmittance) in the second collision cell. The ion products are selected by the electrostatic analyzer (MS-II) and allowed to undergo collisions with helium (30% transmittance) in the fourth field-free region;[15,33] the CAD products are mass-analyzed by the second magnet (MS-III). The reported spectra are averages of 10 (CAD) or 40 (NR) scans. Flash-vacuum-pyrolysis was carried out in a Pyrex tube (length 125 mm, 12 mm i.d.) heated externally with several turns of a heating tape and attached to a glass probe (length 350 mm) extending to the ionization chamber. The compound to be pyrolyzed was sampled from a small glass bulb through a Teflon valve and a glass capillary restriction to prevent back diffusion of products. The residence time in the hot zone was increased by a plug of Pyrex wool loosely inserted at the end of the pyrolyzer tube.

Methyl *tert*-butyl sulfoxide, methyl *n*-propyl sulfoxide, methyl-d_3 *n*-propyl sulfoxide and di-*n*-butyl sulfoxide were prepared from the corresponding sulfides by sodium periodate oxidation[34] and purified by vacuum distillation. Di-*n*-(butyl-3,3-d_2) sulfoxide was prepared by standard procedures as shown in Scheme III. The 2-fold excess of oxirane is essential for a successful preparaton of butanol-3,3-d_2 from CH_3CD_2-MgBr.

Acknowledgment. We thank B. K. Carpenter and B. Leyh for valuable discussions and the National Science Foundation (Grant CHE-8406387) for generous financial support. Instrumentation funds were provided by the National Institutes of Health (Grant GM 16609) and the Army Research Office (Grant DAA L03-86K-0088).

Supplementary Material Available: Tables of CAD spectral data of CH_2SH^+ from $1^{\bullet+}$ and from $HOCH_2CH_2SH$, complete spectral data for Tables I, III, and IV, and a table of MNDO-calculated vibrational frequencies (5 pages). Ordering information is given on any current masthead page.

(33) McLafferty, F. W.; Todd, P. J.; McGilvery, D. C.; Baldwin, M. A. *J. Am. Chem. Soc.* **1980**, *102*, 3360–3363.

(34) Madesclaire, M. *Tetrahedron* **1986**, *42*, 5459–5495.

(35) (a) Holmes, J. L.; Terlouw, J. K. *Org. Mass Spectrom.* **1980**, *15*, 383–396. (b) Holmes, J. L.; Osborne, A. D. *Org. Mass Spectrom.* **1981**, *16*, 236.